Mesoporous Silica Nanoparticles as Drug Delivery Systems for Targeted Inhibition of Notch Signaling in Cancer

Veronika Mamaeva[1], Jessica M Rosenholm[2], Laurel Tabe Bate-Eya[1], Lotta Bergman[2], Emilia Peuhu[1,3], Alain Duchanoy[2], Lina E Fortelius[3], Sebastian Landor[1], Diana M Toivola[3], Mika Lindén[2,*] and Cecilia Sahlgren[1,3]

[1]Turku Centre for Biotechnology, University of Turku and Åbo Akademi University, Turku, Finland; [2]Center for Functional Materials, Department of Natural Sciences, Åbo Akademi University, Turku, Finland; [3]Department of Biosciences, Cell biology, Åbo Akademi University, Turku, Finland

Notch signaling, a key regulator of stem cells, is frequently overactivated in cancer. It is often linked to aggressive forms of cancer, evading standard treatment highlighting Notch as an exciting therapeutic target. Notch is in principle "druggable" by γ-secretase inhibitors (GSIs), inhibitory peptides and antibodies, but clinical use of Notch inhibitors is restricted by severe side effects and there is a demand for alternative cancer-targeted therapy. Here, we present a novel approach, using imagable mesoporous silica nanoparticles (MSNPs) as vehicles for targeted delivery of GSIs to block Notch signaling. Drug-loaded particles conjugated to targeting ligands induced cell-specific inhibition of Notch activity *in vitro* and exhibited enhanced tumor retainment with significantly improved Notch inhibition and therapeutic outcome *in vivo*. Oral administration of GSI-MSNPs controlled Notch activity in intestinal stem cells further supporting the *in vivo* applicability of MSNPs for GSI delivery. MSNPs showed tumor accumulation and targeting after systemic administration. MSNPs were biocompatible, and particles not retained within the tumors, were degraded and eliminated mainly by renal excretion. The data highlights MSNPs as an attractive platform for targeted drug delivery of anticancer drugs with otherwise restricted clinical application, and as interesting constituents in the quest for more refined Notch therapies.

Received 21 December 2010; accepted 1 May 2011; published online 31 May 2011. doi:10.1038/mt.2011.105

INTRODUCTION

Signaling through the Notch receptor constitutes an evolutionary conserved cell–cell communication mechanism in stem cells and is critical for development.[1,2] Mutations in the components of the Notch pathway and aberrant signaling contributes to carcinogenesis in various cancers, including T-cell leukemia (T-ALL) and solid cancers such as breast, prostate, melanoma, colon and various brain cancers.[3,4] Notch cross-talks with other oncogenic pathways and is implicated in therapy resistance of conventional treatment strategies targeting these pathways.[4–6] Furthermore, Notch plays a significant role in tumor angiogenesis.[7] Notch targeted therapy is thus a very promising treatment option and several clinical trials have been launched to test Notch inhibitors efficacy and safety in cancer treatment (http://clinicaltrials.gov/ct2/results?term=notch+inhibitors). In addition, as Notch controls stem cell fate[8,9] and regenerative responses,[1,10] developing targeted strategies for controlling the duration and strength of Notch activity is of therapeutic interest also in regenerative medicine. Despite the availability of efficient Notch inhibitors such as γ-secretase inhibitors (GSIs), peptides[11] or antibodies,[7,12,13] Notch related treatments are currently prevented by considerable side effects.[13–15] GSIs, originally developed to treat Alzheimer's disease, efficiently inhibit Notch[8,16] activation (**Figure 1a**). However, due to the requirement for Notch signaling in most tissues, GSI treatment gives rise to considerable side effects including diarrhea and suppression of lymphopoiesis.[14,15] Intermittent dosing schedules[4,5,17] and possibly co-treatment with glucocorticoids[18] can reduce adverse effects. These approaches, however, are associated with other complications and clinically efficient suppression of Notch activity requires more targeted delivery strategies.

An attractive means for targeted drug delivery is to use drug carriers to which cell-specific targeting ligands have been linked.[19,20] Most GSIs are small, hydrophobic molecules which require vehicles able to carry sufficient amounts of hydrophobic drugs. We have developed mesoporous silica nanoparticles (MSNPs), with a large intrinsic pore volume adequate for high concentrations of cargo, and demonstrated that they are suitable for targeted delivery of hydrophobic model drugs *in vitro*.[21–23] MSNPs can further carry a wide array of drug modalities, making them especially attractive for Notch therapy. The relative ease and flexibility of functionalization of silica allows straightforward covalent linking of cell-specific ligands to the MSNPs. This

The first two authors contributed equally to this work.

***Current address:** Inorganic Chemistry II, University of Ulm, Albert-Einstein-Allee 11, 89081 Ulm, Germany.*
***Correspondence:** Cecilia Sahlgren, Turku Centre for Biotechnology, University of Turku and Åbo Akademi University, P.O. Box 123, FI-20521, Turku, Finland. E-mail: cecilia.sahlgren@btk.fi*

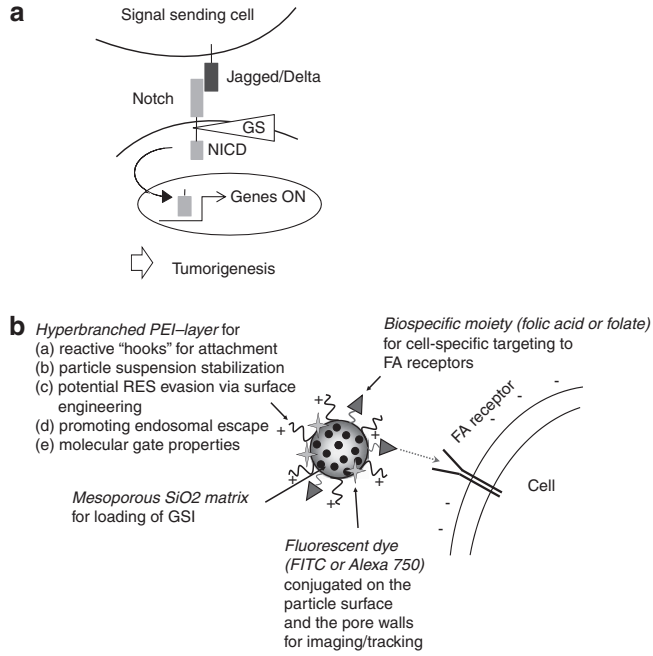

Figure 1 Targeting Notch signaling by design. (**a**) Upon binding to Jagged or Delta ligands, the Notch receptor is subjected to proteolytic processing that releases the Notch intracellular domain (NICD), which translocates to the nucleus where it regulates Notch-dependent gene expression. The cleavage event is mediated by the γ-secretase (GS) complex rendering Notch sensitive to GS-inhibitors (GSIs). (**b**) For targeted Notch therapy, the following particle design was chosen: mesoporous silica nanoparticle (MSNP) matrix for loading of GSI; surface functionalization of a PEI-layer for facilitated further modifications such as coupling of targeting ligands, suspension stabilization, and possible molecular gate properties; labeling with fluorophore for easy visualization and conjugation of folate (FA) to the PEI-layer on the particle surface for cellular targeting. FITC, fluorescein isothiocyanate

flexibility also allows control over parameters, such as particle diameter, shape, charge and pore surface chemistry, that regulate biobehavior and drug release properties.[21,22,24,25] Despite the number of *in vitro* studies by us[21–23,26,27] and others,[24,28] evidences for the biocompatibility, targetability and therapeutic efficiency of drug-containing MSNPs *in vivo* are still largely lacking. As highlighted above, Notch signaling provides an excellent biological system for addressing these questions. In this work, we demonstrate that targeting ligand-conjugated MSNPs are suitable for cell-specific delivery of the GSI DAPT {N-[N-(3,5-Difluorophenacetyl)-L-alanyl]-S-phenylglycine t-butyl ester}. We further confirm tumor retention and targetability *in vivo* and prove enhanced therapeutic efficacy of GSI-loaded MSNPs on tumor reduction and regulation of Notch driven stem cell fates as compared to free drugs *in vivo*. In addition, we show that the particles are biocompatible and biodegradable and provide evidence for the potential of systemic delivery of the developed drug delivery system.

RESULTS

Functionalized MSNPs for GSI delivery

To evaluate targeted delivery of GSIs by MSNPs we synthesized fluorescein isothiocyanate (FITC) (for *in vitro*)- or AlexaFluor750 (for *in vivo*)-labeled polyethylenimine (PEI) MSNPs of an average size centered around either 200 or 350 nm (**Supplementary Figure S1e**). The particles were loaded with the GSI, DAPT (5 weight% or 1 weight%, corresponding to 115 μmol/g and 23 μmol/g, respectively). In order to enable active targeting of the MSNPs to cancer cells, folate (FA) was covalently conjugated to the outer PEI-layer of the particles (See **Figure 1b** for experimental design). The folate receptor (FR) is overexpressed on the surface of a number of different cancer cells, and we have previously shown that FA provides good cancer cell specificity *in vitro*.[23,26,27] Particles were characterized according to standard MSNP characterization methods (**Supplementary Figure S1**). The targetability of the particles were prescreened using cells expressing high (HeLa) or low (293) levels of the FR as models.[23,26,27] FA-conjugated MSNP were specifically taken up by the FR-expressing cells, (**Supplementary Figure S1f**) and were further shown to be noncytotoxic (**Supplementary Figure S1g**) in agreement with our previous results.[23,26,27]

Cell-specific GSI delivery and Notch inhibition by MSNPs

To determine targeted delivery of GSI for cell-specific Notch inhibition, we used a luciferase-based reporter assay (12 × CSL-luciferase) to analyze Notch activity in the FR-low and FR-high cells where Notch had been activated with a gain-of-function version of Notch1, Notch1 ΔE that can be inhibited by GSIs. Notch activity was specifically blocked in a dose-dependent manner in FR-high cells as compared to FR-low cells, in which GSI particles showed no significant effect (**Figure 2a**). These results confirm targeted delivery and cell-specific Notch inhibition, and, importantly, also demonstrate the lack of premature leakage of the drug into the medium as leakage to the medium would have inhibited Notch in FR-low cells. Containment of the drugload within the vehicles was further supported by lack of GSI-release from particles in physiological buffer over a period of 48 hours as determined by high pressure liquid chromatography (**Supplementary Figure S2**). The specific response in FR-high cells to GSI particles was not due to enhanced sensitivity of these cells to GSI, as addition of free GSI inhibited Notch signaling in both cell types to a similar extent (**Figure 2b**). Particle-mediated delivery furthermore significantly enhanced the biological effect as compared to free drug administration with a 50% inhibition obtained by free GSI as compared to more than 80% inhibition with GSI-MSNPs (**Figure 2a,c** box). Further, the inhibition of Notch activity by GSI-MSNPs was stringently dose-dependent as shown in **Figure 2a**. This was further supported by the levels of Notch intracellular domain shown in **Figure 2c** implying that accurate activity control can be achieved by varying either the particle concentration or the concentration of the drug load.

FR-mediated targeting to breast cancer cells

We and others have shown that Notch signaling is upregulated in breast cancer and that GSIs provide a therapeutic benefit.[29–31] To analyze FR-mediated internalization of MSNPs in breast cancer cells, we screened the uptake of FA-conjugated nanoparticles in a range of different breast cancer cell lines (MCF7 (FR-positive), MDA-MB-231, T47D, SK-BR-3, MDA-MB-468) with variable surface levels of the FR (**Figure 3a**). All studied cells internalized FA-tagged particles within 4 hours, although the level of internalization varied between cells (**Figure 3b**). The differences

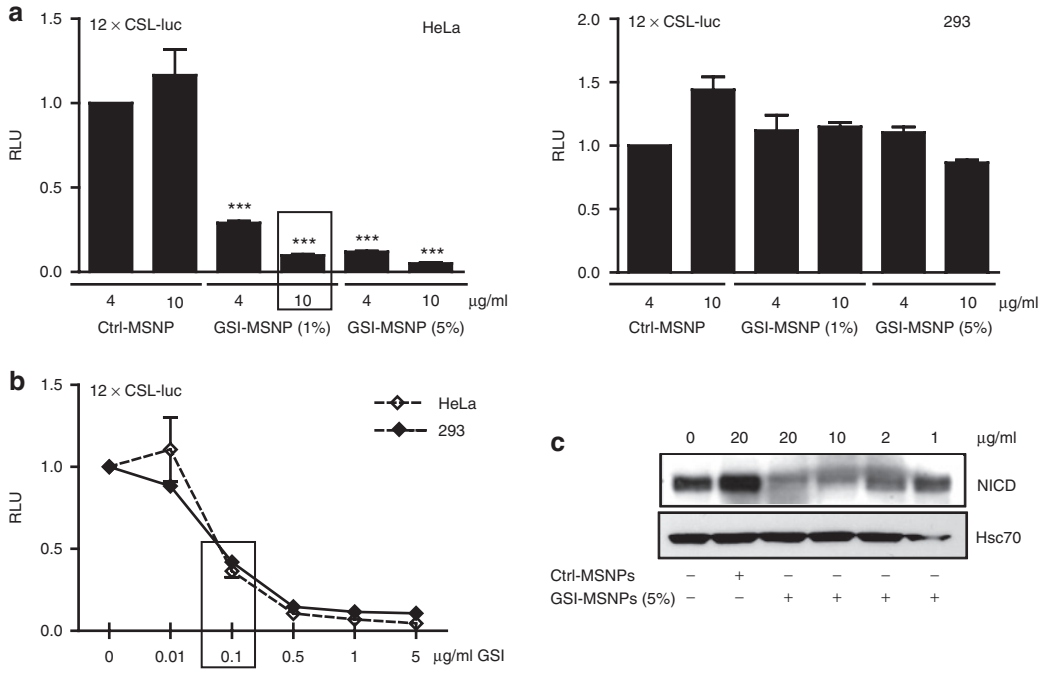

Figure 2 Cell-specific block of Notch signaling by γ-secretase inhibitor-mesoporous silica nanoparticles (GSI-MSNPs) conjugated to folate (FA). (**a**) Luciferase reporter assays for Notch activity demonstrate cell-specific inhibition of Notch in high- folate receptor (FR) HeLa cells as compared to low-FR 293 cells at 24 hours of incubation with MSNPs loaded with 1 weight% and 2.5 weight% GSI, respectively. Notch was activated by transfection of ΔE Notch1 in both cell lines. Control MSNPs (Ctrl-MSNPs) denote drug free control particles; GSI-MSNPs denote GSI-containing particles. Both particles were FA-conjugated. X-axis denotes particle concentration ($n \geq 3$; mean ± SD). (**b**) Luciferase reporter assay demonstrates dose-dependent inhibition of Notch signaling by free GSI in 293 and HeLa cells ($n \geq 3$; mean ± SD). The boxes in **a** and **b** denote GSI concentration at 0.1 µg/ml (***$P < 0.0001$). (**c**) Immunoblot of HeLa cells transfected with GS-cleavable active form of Notch, ΔENotch1, and treated with GSI-loaded (GSI-MSNPs) and drug free particles (Ctrl-MSNPs) using an antibody against the GS-cleaved active form of Notch, Notch intracellular domain (NICD). Hsc-70 is used as a loading control. RLU, relative luciferase units.

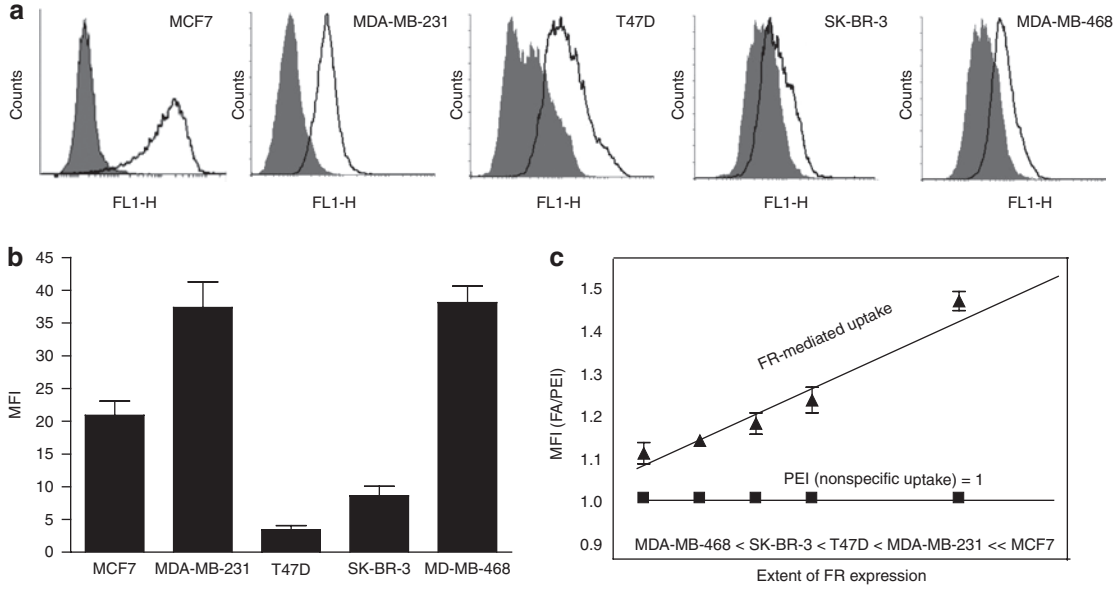

Figure 3 Internalization of folate (FA)-conjugated mesoporous silica nanoparticles (MSNPs) in MCF7 (FA high), MDA-MB-231, T47D, SK-BR-3 and MDA-MB-468 breast cancer cells. (**a**) Folate receptor (FR) surface expression in breast cancer cells. Cells were labeled with anti-FR antibody followed by Alexa 488-conjugated secondary antibody (black line) and analyzed by flow cytometry. Nonspecific fluorescence was measured using the secondary antibody only (shaded area). The results are representative of two independent experiments. (**b**) The endocytosed particles were detected by flow cytometry and mean fluorescence intensity (MFI) was measured after 4 hours and normalized to background fluorescence of each cell line in the absence of particles ($n = 3$, mean ± SD). (**c**) FA-mediated uptake of MSNPs. Uptake of PEI-MSNPs and FA-MSNPs was measured at 4 hours of particle incubation and normalized to background fluorescence. The graph shows the FA-mediated uptake as a function of the unspecific uptake of FA-MSNPs ($n = 3$, mean ± SD).

in uptake most likely reflect cell-specific differences, *i.e.*, cell morphology, surface area, and endocytosis rate and mechanisms, rather than the level of receptors on the surface. To assess the significance of active (FA-mediated) targeting, we measured endocytosis of FA-MSNPs and PEI-MSNPs. When the uptake of FA-MSNPs was plotted as a function of the uptake of PEI-MSNPs (nonspecific uptake) the FR-mediated internalization correlated well with the surface levels of the FR on the different cells (**Figure 3a,c**). The FA-mediated endocytosis was highest in MCF7, in agreement with recent data demonstrating efficient FA-mediated uptake in MCF7 cells,[32] and in MDA-MB-231 cells expressing high levels of the receptor. FR-mediated internalization was further supported by competition experiments with free FA (**Supplementary Figure S3a**) and by the observation that FA-tagging of the MSNPs facilitated cellular uptake (as measured by % of cells and amount of internalized particles) only in cells expressing the FR (**Supplementary Figure S3b**). Taken together, the correlation of FA-facilitated uptake with receptor levels and inhibition of FA-mediated uptake by free ligand competition,[23] are in favor of particle internalization through FR-mediated endocytosis.

Targeting enhances tumor penetration and retains MSNPs at the tumor site *in vivo*

Tumor accumulation of nanoscopic drug carriers *in vivo* is facilitated by the combination of passive and active targeting. The main objective of active targeting, is to enhance interactions with tumor cells to facilitate cellular uptake and retain the drug carrier within the tumor. To verify active targeting *in vivo*, we analyzed the behavior of FA-MSNPs, as compared to nontargeted PEI-MSNPs after peritumoral (p.t.) injections in nude mice bearing subcutaneous MDA-MB-231 tumors. Incorporation of a far-red fluorophore into MSNPs provided an efficient tracking system to follow the fate of the particles *in vivo.* To ensure that the fluorescent signal from PEI-MSNPs and FA-MSNPs was comparable all used particle batches were prescreened for signal to concentration ratio before use (**Supplementary Figure S4a**). After p.t. injections (20 mg/kg) we observed enhanced retainment and increased tumor penetration of FA-MSNPs as compared to PEI-MSNPs (**Figure 4a,b**). This result was further verified by *ex vivo* analyses of isolated tumors (**Figure 4c**). Hence, improved tumor retention and penetration of MSNPs *in vivo* were achieved through conjugation of targeting ligands also *in vivo*.

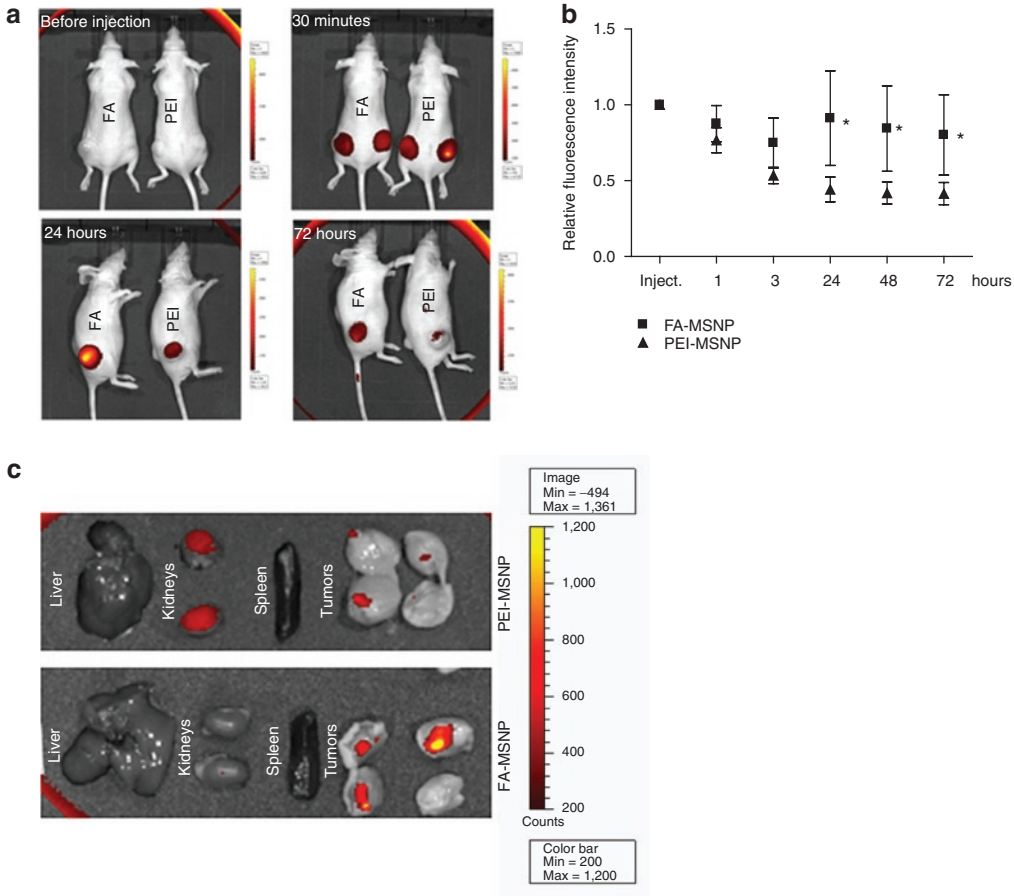

Figure 4 Tumor accumulation and retention of mesoporous silica nanoparticles (MSNPs) through folate (FA)-functionalization. (**a**) FA-conjugated and nonconjugated particles (PEI) were injected peritumorally and followed by the IVIS Lumina II imaging system for 72 hours. Scale bars range from 300 to 8000 counts for images 30 minutes to 72 hours, whereas scale bar is 200 to 4500 counts for control image (before injection). (**b**) Graph shows the quantification of the fluorescence intensity in tumors injected with FA-MSNPs and PEI-MSNPs over time as related to the initial intensity within each tumor ($n = 6$, two tumors per animal). (*$P < 0.05$). (**c**) *Ex vivo* imaging of internal organs and tumors 72 hours after injection of MSNPs. The tumors were cut in half to visualize particles within the tumor tissue.

GSI-loaded MSNPs show enhanced Notch inhibition as compared to free drug *in vivo*

In order to validate the applicability of MSNPs for delivery of GSIs *in vivo*, we tested GSI-loaded FA-tagged particles (GSI-MSNPs) for therapeutic efficacy in mice bearing MDA-MB-231 tumors. It has previously been shown by Rizzo *et al.*[6] that MDA-MB-231 cells have high intrinsic Notch activity and that treatment of mice with MDA-MB-231 tumors by p.t. injections of 1.2 mg/kg GSI every second day for 2 weeks for the whole course of the experiment reduced tumor growth. As particle-mediated GSI delivery enhanced the therapeutic efficacy *in vitro* (**Supplementary Figure S5**) we used an alternative administration scheme were particles (1 mg/kg GSI) were injected every 3rd day for 12 days when the treatment was terminated and the mice left untreated for an additional 2 weeks. Treatment with GSI-loaded particles clearly reduced tumor growth and the effect was detectable even 2 weeks after the last injection (**Figure 5a**). The same administration regime of free GSI had no effect on tumor growth (**Figure 5b**). The levels of Notch intracellular domain were clearly reduced in tumors treated with GSI-loaded particles as compared to tumors treated with control particles determined by western blotting, demonstrating inhibition of Notch activity (**Figure 5c**). Notch signaling plays an essential role in intestinal morphogenesis and homeostasis, and blockade of Notch signals results in the arrest of crypt cell proliferation and converts crypt cells into a goblet cell fate[14,33,34] In line with the role of Notch governing cell fate decision in the gastrointestinal tract, the most prominent effect of chronical administration of GSIs is diarrhea. Efficient drug delivery to colon tissues through oral administration is counteracted by nonspecific adsorption along the delivery route and the acidic environment of the stomach. To test whether MSNPs could provide a drug carrier system for oral delivery of GSIs, FVB/N adult mice were fed by oral gavage once a day for 3 days with free GSI at a concentration of 500 mg/kg and GSI-MSNPs at a concentration of 200 mg/kg (GSI 2 weight%) and monitored for signs of diarrhea and analyzed for Notch-mediated cell fate switches in the gastrointestinal tract. As control for particle-mediated effects one group of mice were treated with unloaded control MSNPs (Ctrl-MSNPs). After 3 days the GSI- and GSI-MSNP-treated mice showed clear diarrhea (**Figure 5d**), the % change of stool hydration was 20 for free GSI (500 mg/kg) and 32 (200 mg/kg) for GSI-MSNPs demonstrating a clearly enhanced effect by MSNPs-mediated delivery. Histochemical examination demonstrated intestinal goblet cell differentiation in line with the expected effects of Notch inhibition and the effect was enhanced after treatment with GSI-MSNPs as compared to treatment with Ctrl-MSNPs (**Figure 5e**). Taken together, we show efficient MSNPs mediated-GSI-delivery and Notch inhibition *in vivo* by two different administration routes, p.t. injections and oral administration and the therapeutic efficacy of particle-mediated delivery was significantly enhanced as compared to free drug administration in both cases.

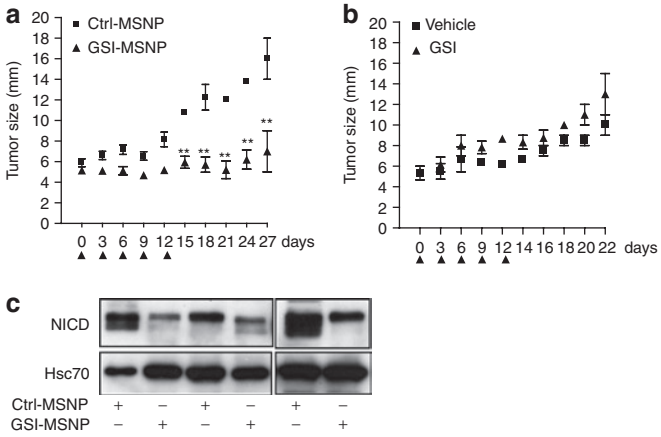

d

Treatment	Control	GSI	Ctrl-MSNP	GSI-MSNP
% Stool hydration ± SD	60.33 ± 7.3	80.9 ± 3.5	50.9 ± 6.5	82.1 ± 4.6
Relative stool wet weight	1	1.3	1	1.6
n	3	3	2	4
P value	<0.05		<0.002	

e

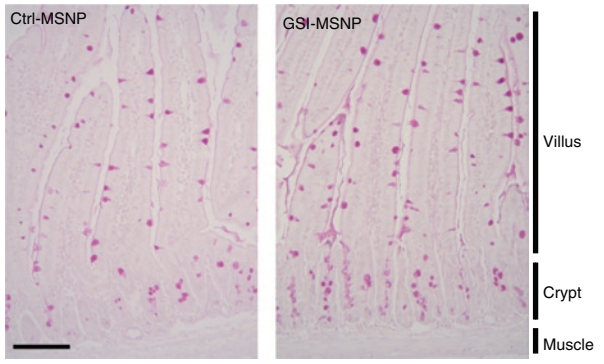

	Goblet cells/villus		Goblet cells/crypt	
Treatment	Ctrl-MSNP	GSI-MSNP	Ctrl-MSNP	GSI-MSNP
Average ± SD	17.2 ± 4.7	19.3 ± 6.2	4.7 ± 2.2	6.2 ± 2.2
n	48	70	173	169
P value	<0.05		<0.0002	

Figure 5 γ-Secretase inhibitor (GSI)-loaded mesoporous silica nanoparticles (MSNPs) block Notch activity, inhibit tumor growth, and control stem cell functions *in vivo*. (**a**) MDA-MB-231 tumor-bearing mice were injected peritumorally up to day 12 (arrowheads) with FA-conjugated GSI-loaded (GSI-MSNP, 20 mg/kg, 2.5 weight% GSI) and empty MSNPs [control MSNPs (Ctrl-MSNP), 20 mg/kg] (tumor size was followed for 3 weeks ($n = 6$, mean ± SD). (**$P < 0.011$). (**b**) MDA-MB-231 tumor-bearing mice were injected peritumorally up to day 12 (arrowheads) with 1 mg/kg free DAPT {N-[N-(3,5-Difluorophenacetyl)-L-alanyl]-S-phenylglycine t-butyl ester} (GSI) or the DMSO aqueous vehicle solution (Vehicle). Tumor size was followed until day 22 ($n = 4$, mean ± SD). (**c**) GSI-MSNP-treatment leads to reduction in the levels of active Notch in the tumors, as demonstrated by western blot using an antibody against Notch intracellular domain (NICD), the active form of Notch. (**d**,**e**) Oral delivery of GSI-MSNP induces goblet cell differentiation and diarrhea. (**d**) Stool from mice fed by gavage with DMSO-vehicle solutions, free DAPT (500 mg/kg), control particles (Ctrl-MSNP) and DAPT particles (GSI-MSNP, 250 mg/kg DAPT) (2–4 mice per treatment) was collected. The % water content (stool hydration) was determined from stool wet and dry weights. Statistics; Students *t*-test, unpaired, normal distribution. (**e**) Duodenum from mice fed control particles (Ctrl-MSNP) or GSI particles (GSI-MSNP) by gavage (2 mice per treatment) was excised, fixed in 4% paraformaldehyde and processed for paraffin embedding. 6 µm sections were stained for Goblet cells by Periodic-Shiff (PAS)-staining, and the number of goblet cells in intact crypts and villi displaying clear cross sections were counted in 6–10 sections per mice. Statistics; Students *t*-test.

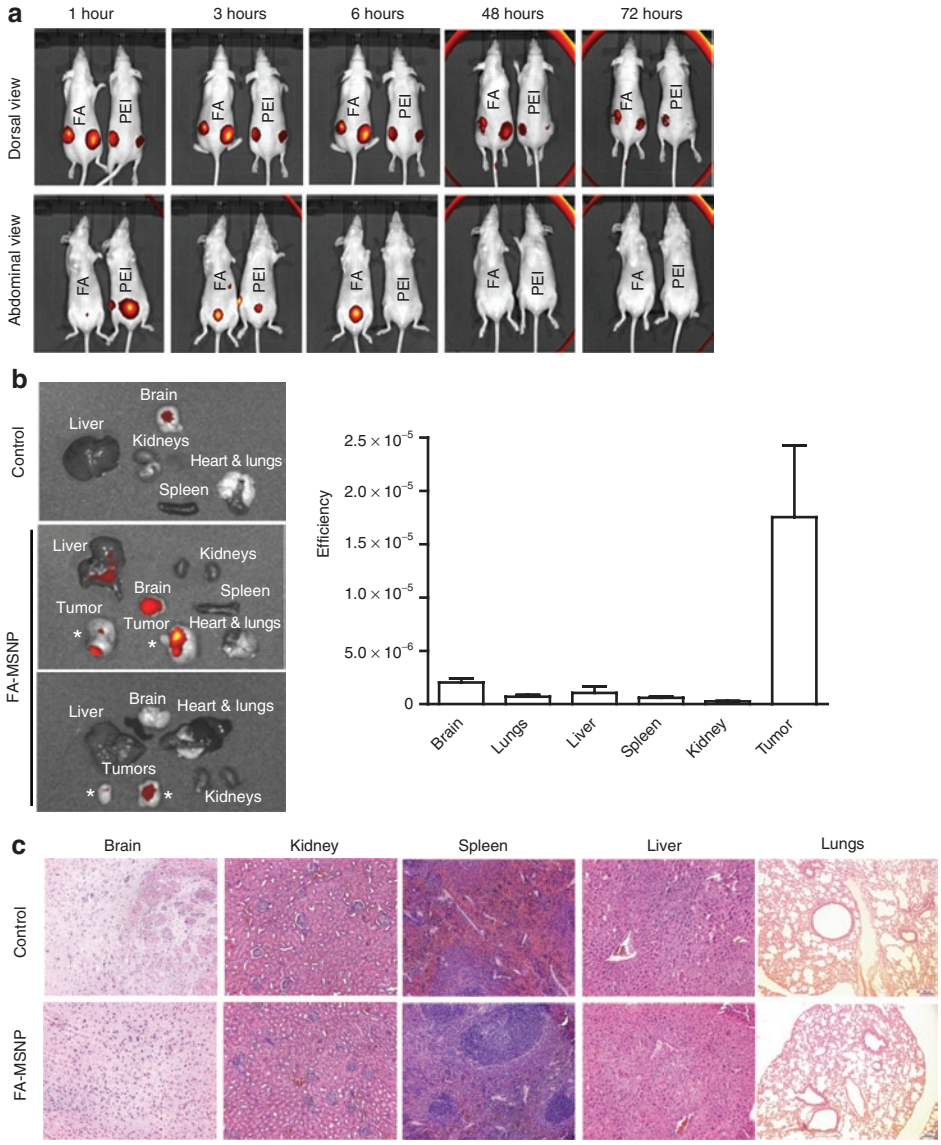

Figure 6 Mesoporous silica nanoparticles (MSNPs) accumulate in the tumors, are biocompatible biodegradable and eliminated through renal excretion. (**a**) *In vivo* imaging of mice injected peritumoral with PEI-MSNPs or folate (FA)-MSNPs. Images of the abdominal area demonstrate accumulation of fluorescence in the bladder, and imaging of the dorsal area show accumulation of fluorescence in the tumors. Time lapse imaging of the abdominal area shows elimination of fluorescence within 48 hours after injections (number of animals per group, $n = 4$, two tumors per animal). (**b**) *Ex vivo* analyses (left) and quantification of fluorescence intensity (right) in organs from mice injected intravenous (i.v.) with FA-MSNPs. Mice were killed 196 hours after injection ($n = 4$). Please note the occasional signal from brain tissue which most likely represents background fluorescence as it is present also in untreated control animals. (**c**) Histological analysis of brain, kidney, spleen, liver, and lungs of untreated mice and FA-MSNPs-treated mice showed no morphological changes. Mice were killed 192 hours after i.v. injection.

MSNPs are biocompatible, biodegradable and can be targeted to tumors upon i.v. administration

In order to evaluate the biocompatibility of the developed MSNPs, we followed the particles after both p.t. (**Figure 6a**) and intravenous (i.v.) (**Figure 6b,c**, **Supplementary Figure S6**) administration. Within a few hours after p.t. injection of particles (20 mg/kg), a strong fluorescent signal was visible in the bladder indicating urine excretion of non-retained particles (**Figure 6a**). At 48 hours, the signal in the bladder was below the detection limit (**Figure 6a**) indicating that the majority of particles which were not internalized by cancer cells were eliminated within 2 days. This is in agreement with the dissolution kinetics of silica in biological buffer, demonstrating a 70% dissolution rate at 50 hours (**Supplementary Figure S6a**). Inductively coupled plasma optical emission spectrometry analyzes of the silica content in urine collected from mice injected i.v. with FA-MSNPs at 4 and 24 hours further supported biodegradation and renal excretion (**Supplementary Figure S6b**). On the contrary, internalized particles are dissolved at a slower rate[26] and at 72 hours after injection FA-conjugated particles were still present in tumors in line with efficient cancer cell internalization. After i.v. injections (20 mg/kg) we observed tumor accumulation within 12 hours after injection and particles were still clearly visible at the tumor site at 120 hours (**Supplementary Figure S7a**). Specific tumor accumulation was further supported by *ex vivo*

analyses of isolated organs at 196 hours after particle administration (**Figure 6b** and **Supplementary Figure S7b**). To analyze the significance of active targeting, we quantified the signal at 72 hours after injection *ex vivo* in organs of animals that had been injected i.v. with PEI-MSNPs and FA-MSNPs. Although FA-MSNPs showed slightly enhanced accumulation PEI-MSNPs also were preferably localized to tumors (**Supplementary Figure S7c**). FA- and PEI-MSNPs otherwise showed quite similar distribution at 72 hours after injection and both particles appeared to be biodegradable and eliminated with the exception of accumulation of FA-tagged particles in the lungs (**Supplementary Figure S7c**). At 196 hours, the signal from the lungs in mice that had been injected with FA-MSNPs was no longer detectable (**Figure 6b**), implying that although FA-conjugated particles showed lung accumulation at 3 days after injection (**Supplementary Figure S7c**) particles were degraded and eliminated within 8 days.

In agreement with efficient elimination of particles, mice treated with FA-MSNPs demonstrated no pathological abnormalities in major organs (**Figure 6d**) at 8 days after i.v. administration and gross histology of brain, liver, spleen, kidneys and lungs isolated from treated and control mice was identical (**Figure 6c**). The animals tolerated particle treatment well. Body weight did not change during treatment, and no reduced food intake, impaired mobility nor were visible infections observed (data not shown), indicating high biocompatibility of MSNPs. Irrespective of the administration route, the mice lacked any signs of systemic inflammatory responses as determined by serum levels of interleukin-6 and tumor necrosis factor-α (**Supplementary Figure S8a**). As the kidneys and urine excretion appeared to be the main route of elimination, we analyzed kidney function by measuring serum creatinine levels in untreated mice and of mice treated with PEI-MSNPs or FA-MSNPs. We observed no significant elevation of creatinine levels indicating that the kidney function was not impaired (**Supplementary Figure S8b**).

DISCUSSION

Despite the availability of efficient Notch inhibitors, such as GSIs, the requirement of Notch in maintaining homeostasis in most tissues prevents general Notch inhibition. To circumvent adverse effects, better drug delivery platforms for localized Notch inhibition need to be developed. MSNPs have attracted immense interest in the biomedical field as vehicles for targeted delivery, but there is very limited knowledge of their therapeutic applicability and biocompatibility *in vivo.* Here, we show that MSNPs provide a novel platform for efficient GSI delivery *in vivo* highlighting MSNPs as valuable constituents in the development of intelligent Notch therapeutics. Despite ongoing efforts to develop more targeted Notch therapies,[7,12–14] this is the first report demonstrating successful targeted vehicle-mediated delivery of Notch inhibitors with significantly improved therapeutic efficacy as compared to free drug *in vivo*.

The most critical question regarding the use of MSNPs for therapy is its actual efficacy for delivering drugs through different administration routes. To our knowledge, there is only one recent study demonstrating tumor-suppressing activity *in vivo* by camptothecin containing MSNPs.[32] Here, we demonstrate that GSI-MSNPs efficiently blocked Notch signaling and tumor growth in mouse xenograft models upon p.t. administration and induced goblet cell metaplasia as a consequence of Notch inhibition upon oral delivery. MSNPs-mediated GSI delivery provided a significant therapeutic benefit over free drug administration, which was virtually noneffective at inhibiting tumor growth, allowing the use of lower concentration and less frequent dosing. This is encouraging as using MSNPs as delivery vehicles for GSI, or any other drug, especially those related to severe side effects, may allow for the use of drug concentrations below the toxicity limit. Although we used GSIs as a model for Notch inhibition, the platform can be adopted for delivery of other drug classes[22,26] including antibodies[12] and peptides[11] that constitute recent developments of Notch therapeutics. Further, Notch cross-talks extensively with other pathways[4–6,35] that include candidate therapeutic targets, which also makes strategies to use combinatorial treatments an interesting avenue. Such treatments could be accomplished with high precision using the nanoparticle technology platform where the optimum particle-cargo combinations can be rationally chosen.

Our data show tumor accumulation and retainment *in vivo*, although also nontargeted particles accumulate at tumor sites after i.v. administration. This is most likely due to passive targeting due to the leaky vascular of tumors, known as the enhanced permeability and retention effect.[36] FA-tagged particles were retained longer in the tumor area indicative of efficient cellular internalization, in line with our previous data on particle stability inside cells.[26] Here we used FA as the targeting moiety, although the flexibility of the MSNP-based drug delivery system enables easy modifications of the particles with other types of targeting ligands, such as antibodies,[37] peptides, and aptamers,[38] which can be easily linked to MSNPs, providing a platform for more individual-based targeting strategies.

The biocompatibility of MSNPs will depend on morphology, size, composition and surface chemistry in addition to the dosage and the administration route used. FA-PEI and PEI-modified particles at the concentrations used in this study (20 mg/kg) were well tolerated irrespective of the route of administration. In agreement with the absence of adverse effects, particles that were not targeted to the tumors appeared to be efficiently eliminated from the body primarily by renal excretion. This is in agreement with previous reports on MSNPs showing that renal clearance was the major route of excretion although these authors used different MSNPs with different sizes and surface modifications.[32,39] These reports also show that size critically affect the circulation time. Future work need to be focused at optimizing the technology with regards to circulation time, drug release kinetics in order to obtain the optimal particle for i.v. administration, the preferred administration route. Modulation of size and surface properties of MSNPs allow for optimization of the pharmacokinetics of the delivery platform. For example, a recent publication demonstrated that surface charge influenced hepatobiliary excretion of MSNPs.[40] Detailed understanding of how different modifications of MSNPs influence biobehavior *in vivo* will need to be the focus of future studies for medical applicability of the technology.

Taken together, the incorporation of Notch modifiers into MSNPs presents a novel approach in the development of refined Notch therapy. Based upon the example of the Notch signaling pathway, the data demonstrate that MSNPs is a promising

platform for targeted therapeutic approaches and enhanced therapeutic efficacy in cancer.

MATERIALS AND METHODS

Preparation and characterization of MSNPs. Amino-functionalized co-condensed MSNPs were synthesized according to previously described[41] but with the thiol-silane replaced by 3-aminopropyltrimethoxysilane in accordance with our earlier publication.[23] For more detailed description on synthesis, drug loading and characterization of the particles please see the **Supplementary Materials and Methods**.

Cell culture and assessment of particle endocytosis and cellular toxicity. All cell lines were obtained from ATCC, Manassas, VA. HeLa cervical carcinoma cells, HEK 293 (human embryonic kidney) cells and breast cancer cell lines, T47D, MDA-MB-231, SK-BR-3, MDA-MB-468, MCF7, were cultured on 12-well plates in Dulbecco's modified Eagle's medium (Sigma, St Louis, MO) supplemented with 10% fetal calf serum (BioClear, Calne, UK), 2 mmol/l L-glutamin, 100 U/ml penicillin, 100 g/ml streptomycin in 37 °C and 5% CO_2. For particle handling, anlayses of particle endocytosis by flow cytometry see ref. 23. For FA competition experiments the cells were cultured overnight with 1 mmol/l folic acid (Sigma) prior to addition of the particles. MSNPs were suspended in growth medium at a concentration of 10 μg/ml. After 20-minute sonication in water bath, the medium with particles or the control medium was added to the 50–70% confluent cells and incubated for 4 hours at 37 °C. The cells were trypsinized and the extracellular fluorescence was quenched by resuspension to 200 μg/ml trypan blue (Fluka, St Louis, MO) for 5 minutes at room temperature. The cells were washed once and resuspended in phosphate-buffered saline. The amount of endocytosed particles inside cells was analyzed by FacsCalibur flow cytometer (BD Pharmingen, San Diego, CA). The mean fluorescence intensity of the cells at FL-1 channel was measured. The data were analyzed with Cyflogic software. For assessment of apoptotic cell death, the cells were incubated in the presence of 10 μg/ml nanoparticles for 72 hours. For cytotoxicity analysis the cells were collected by trypsinization and resuspended in propidium iodide buffer (40 mmol/l Na-citrate, 0,3% Triton X-100, 50 μg/ml propidium iodide; Sigma). After 10-minute incubation, the samples were analyzed for nuclear fragmentation with FacsCalibur flow cytometer (FL-2, BD Pharmingen). The fraction of sub-G0/G1 events (nuclear fragmentation) was detected as a measure of apoptotic cell death.

Activation of Notch signaling and assessment of Notch signaling activity. The ΔENotch1 construct and the 12 × CSL-luciferase reporter construct has previously been described.[31] HeLa and 293 cells were co-transfected with ΔENotch1 for activation of Notch signaling, and 12 × CSL-luciferase and B-gal constructs for measuring Notch signaling activity. Twenty-four hours after transfection GSI-loaded particles (GSI-MSNPs) and corresponding GSI-free control particles (Ctrl-MSNPs) dissolved in Hepes buffer were added to the cells at denoted concentrations. After 24 hours, the cells were lysed and Notch signaling was determined by luciferase assay, as previously described.[31] For ligand activation, HeLa cells expressing the full length Notch receptor were cocultured with 3T3 cells expressing the Notch ligand Jagged or control cells lacking expression of the ligand. Receptor-expressing cells were pretreated with MSNPs for 4 hours whereafter the medium was removed, cells were washed three times and the medium was replaced with medium containing ligand-expressing cells. After 48 hours of co-culture the cells were lysed in Promegas passive lysate buffer for luciferase assay.

Animals. All animal experiments were conducted in accordance with the institutional animal care policies of the University of Turku/Åbo Akademi University (Turku, Finland). Athymic Nude-Foxn1nu 5-to 6-week-old female mice (Harlan, Horst, Netherlands) were housed in Scantainer cages (Tecniplast, Buguggiate, Italy) three to five per cage supplied with TD.97184 chlorophyll-free mouse chow (Harlan Teklan, Madison, WI) and tap water *ad libitum*, in controlled conditions of light and temperature. To initiate tumors, mice were injected subcutaneously into both flanks with 1×10^6 MDA-MB-231 cells in the presence of Matrigel (BD Biosciences, Franklin Lakes, NJ) and kept until tumors reached ~100 mm^3. Biodistribution of FA- or polyethyleneimine-PEI functionalized (see **Supplementary Figure S1**) MSNPs (20 mg/kg) was followed up in mice after i.v. injection in the tail vein. Images were obtained with IVIS Lumina II (Caliper Life Sciences, Hopkinton, MA) with a combination of 745 nm excitation filter and indocyanine green emission filter at various time points after injection. For assessment of the effect of MSNPs on tumor growth, tumor-bearing mice were injected peritumorally (in the vascular bed of the tumor) with (i) FA-tagged GSI-containing MSNPs (GSI-MSNPs, 20 mg/kg, weight 2.5% DAPT) (ii) Ctrl-MSNPs (20 mg/kg), (iii) free DAPT (1 mg/kg,), and (iv) vehicle-HEPES. Frequency of injections was once every 3rd day. Treatment was terminated at day 12 after first injection, and mice were followed up for an additional 15 (all MSNPs) and 10 (DAPT and vehicle) days. Tumor diameter was determined by vernier caliper every third day.

To demonstrate active targeting mechanism, FA-conjugated (FA-MSNPs) and nonconjugated particles (PEI-MSNPs) (20 mg/kg) were injected peritumorally and the distribution of particles was followed during 72 hours. Fluorescence intensity was determined with Living Image 3.1 software from anatomical (drawn around tumor) regions of interests. The results were presented as fluorescence intensity over time related to the initial intensity within each tumor ($n = 4$, two tumors per animal). At the end of all treatments animals were killed, and tumors, liver, kidneys, spleen, lungs, and brain were removed, imaged *ex vivo* and fixed in 4% paraformaldehyde for histological analyzes, or snap frozen in liquid nitrogen for western blotting. The serum levels of inflammatory cytokines were analyzed with mouse IL-6 immunoassay kit (Invitrogen, Carlsbad, CA) and mouse TNF-α Instant ELISA kit (Bender MedSystems, Hatfield, UK) according to manufacturer's instructions. Kidney function was assessed with serum creatinine detection kit (Arbor assays, Ann Arbor, MI) according to the manufacturers' instructions.

Oral delivery of GSI-MSNP and evaluation of diarrhea. FVB/N adult mice were fed by oral gavage once a day for 3 days with ~350 nm DAPT particles (GSI-MSNPs, 200 mg/kg DAPT), control particles (Ctrl-MSNPs, 250 mg/kg, GSI 2.5 weight%), free DAPT (500 mg/kg), and dimethyl sulfoxide-vehicle solutions. Total volume of administered substances was 0.5 ml per day. Stool samples (2–4 mice per treatment) were collected directly from the animals, weighed, and dried overnight on the heating plate and the water content (% hydration) was determined by the loss of weight upon drying.[15] Goblet cell numbers were analyzed by PAS-staining and light microscopy.

Histological analysis. Organs were collected in 4% paraformaldehyde, fixed overnight in +4 °C, placed in 70% ethanol, and sent for paraffin embedding, sectioning, and hematoxylin-eosin staining (Department of Forensic Medicine, University of Turku). Slides were reviewed in blind by a board-certified pathologist.

Statistical analysis. The cell culture experiments were done a minimum of three times. One-way analysis of variance or *t*-test (GraphPad Prism software, San Diego, CA) was used to determine statistical significance for the following experiments: serum interleukin-6 and tumor necrosis factor concentration measurements, FA competition experiments, luciferase activity, and fluorescence intensity in regions of interest, goblet cell numbers.

SUPPLEMENTARY MATERIAL

Figure S1. MSNP characterization.
Figure S2. DAPT-release from MSNPs as measured by HPLC.
Figure S3. FR-mediated targeting of FA-tagged MSNPs.
Figure S4. Fluorescent intensity of FA-MSNPs and PEI-MSNPs.
Figure S5. Successful Notch inhibition in MDA-MB-231 cells by GSI-MSNPs.

Figure S6. Mesoporous silica nanoparticles are degradable.
Figure S7. Tumor accumulation and biodistribution of MSNPs after i.v adminsitration.
Figure S8. MSNPs does not induce inflammatory reaction nor affect kidney function.
Materials and Methods.

ACKNOWLEDGMENTS

Tommy Nyman is acknowledged for technical assistance. The Department of Pathology, University of Turku is acknowledged for histological analysis. The Cell Imaging Core at the Turku centre for Biotechnology is acknowledged for technical assistance. Dr Hemming is acknowledged for HPLC analysis. The financial support from the Academy of Finland Grants 128477 (E.P.) and 131034 (C.S.), 126161 (D.T.) The Finnish Cancer Organizations (C.S. and V.M). and Sigrid Juselius foundations (C.S. and V.M. and (L.T.B.-E.), the European Union (NanoEar project) (J.R.) and the partial financial support from the Tor, Joe, and and Pentti Borg foundation and Åbo Akademi cancer funds are gratefully acknowledged. ICP-OES analyses were performed at the department of Analytical Chemistry, Åbo Akademi University.

REFERENCES

1. Androutsellis-Theotokis, A, Leker, RR, Soldner, F, Hoeppner, DJ, Ravin, R, Poser, SW *et al.* (2006). Notch signalling regulates stem cell numbers *in vitro* and *in vivo*. *Nature* **442**: 823–826.
2. Artavanis-Tsakonas, S, Rand, MD and Lake, RJ (1999). Notch signaling: cell fate control and signal integration in development. *Science* **284**: 770–776.
3. Radtke, F and Raj, K (2003). The role of Notch in tumorigenesis: oncogene or tumour suppressor? *Nat Rev Cancer* **3**: 756–767.
4. Rizzo, P, Osipo, C, Foreman, K, Golde, T, Osborne, B and Miele, L (2008). Rational targeting of Notch signaling in cancer. *Oncogene* **27**: 5124–5131.
5. Miele, L (2008). Rational targeting of Notch signaling in breast cancer. *Expert Rev Anticancer Ther* **8**: 1197–1202.
6. Rizzo, P, Miao, H, D'Souza, G, Osipo, C, Song, LL, Yun, J *et al.* (2008). Cross-talk between notch and the estrogen receptor in breast cancer suggests novel therapeutic approaches. *Cancer Res* **68**: 5226–5235.
7. Ridgway, J, Zhang, G, Wu, Y, Stawicki, S, Liang, WC, Chanthery, Y *et al.* (2006). Inhibition of Dll4 signalling inhibits tumour growth by deregulating angiogenesis. *Nature* **444**: 1083–1087.
8. Kopan, R and Ilagan, MX (2009). The canonical Notch signaling pathway: unfolding the activation mechanism. *Cell* **137**: 216–233.
9. Miele, L, Golde, T and Osborne, B (2006). Notch signaling in cancer. *Curr Mol Med* **6**: 905–918.
10. Delaney, C, Heimfeld, S, Brashem-Stein, C, Voorhies, H, Manger, RL and Bernstein, ID (2010). Notch-mediated expansion of human cord blood progenitor cells capable of rapid myeloid reconstitution. *Nat Med* **16**: 232–236.
11. Moellering, RE, Cornejo, M, Davis, TN, Del Bianco, C, Aster, JC, Blacklow, SC *et al.* (2009). Direct inhibition of the NOTCH transcription factor complex. *Nature* **462**: 182–188.
12. Wu, Y, Cain-Hom, C, Choy, L, Hagenbeek, TJ, de Leon, GP, Chen, Y *et al.* (2010). Therapeutic antibody targeting of individual Notch receptors. *Nature* **464**: 1052–1057.
13. Yan, M, Callahan, CA, Beyer, JC, Allamneni, KP, Zhang, G, Ridgway, JB *et al.* (2010). Chronic DLL4 blockade induces vascular neoplasms. *Nature* **463**: E6–E7.
14. van Es, JH, van Gijn ME, Riccio O, van den Born M, Vooijs M, Begthel H, *et al.* (2005). Notch/gamma-secretase inhibition turns proliferative cells in intestinal crypts and adenomas into goblet cells. *Nature* **435**, 959–963.
15. Wong, GT, Manfra, D, Poulet, FM, Zhang, Q, Josien, H, Bara, T *et al.* (2004). Chronic treatment with the gamma-secretase inhibitor LY-411,575 inhibits beta-amyloid peptide production and alters lymphopoiesis and intestinal cell differentiation. *J Biol Chem* **279**: 12876–12882.
16. Bray, SJ (2006). Notch signalling: a simple pathway becomes complex. *Nat Rev Mol Cell Biol* **7**: 678–689.
17. Cullion, K, Draheim, KM, Hermance, N, Tammam, J, Sharma, VM, Ware, C *et al.* (2009). Targeting the Notch1 and mTOR pathways in a mouse T-ALL model. *Blood* **113**: 6172–6181.
18. Real, PJ, Tosello, V, Palomero, T, Castillo, M, Hernando, E, de Stanchina, E *et al.* (2009). Gamma-secretase inhibitors reverse glucocorticoid resistance in T cell acute lymphoblastic leukemia. *Nat Med* **15**: 50–58.
19. Davis, ME, Chen, ZG and Shin, DM (2008). Nanoparticle therapeutics: an emerging treatment modality for cancer. *Nat Rev Drug Discov* **7**: 771–782.
20. Ferrari, M (2005). Cancer nanotechnology: opportunities and challenges. *Nat Rev Cancer* **5**: 161–171.
21. Rosenholm, JM, Sahlgren, C and Linden, M (2010). Cancer-cell targeting and cell-specific delivery by mesoporous silica nanoparticles. *J Mater Chem* **20**: 2707–2713.
22. Rosenholm, JM, Sahlgren, C and Lindén, M (2010). Towards multifunctional, targeted drug delivery systems using mesoporous silica nanoparticles–opportunities & challenges. *Nanoscale* **2**: 1870–1883.
23. Rosenholm, JM, Meinander, A, Peuhu, E, Niemi, R, Eriksson, JE, Sahlgren, C *et al.* (2009). Targeting of porous hybrid silica nanoparticles to cancer cells. *ACS Nano* **3**: 197–206.
24. Liong, M, Angelos, S, Choi, E, Patel, K, Stoddart, JF and Zink, JI (2009). Mesostructured multifunctional nanoparticles for imaging and drug delivery. *J Mater Chem* **19**: 6251–6257.
25. Slowing, II, Vivero-Escoto, JL, Wu, CW and Lin, VS (2008). Mesoporous silica nanoparticles as controlled release drug delivery and gene transfection carriers. *Adv Drug Deliv Rev* **60**: 1278–1288.
26. Rosenholm, JM, Peuhu, E, Bate-Eya, LT, Eriksson, JE, Sahlgren, C and Lindén, M (2010). Cancer-cell-specific induction of apoptosis using mesoporous silica nanoparticles as drug-delivery vectors. *Small* **6**: 1234–1241.
27. Rosenholm, JM, Peuhu, E, Eriksson, JE, Sahlgren, C and Lindén, M (2009). Targeted intracellular delivery of hydrophobic agents using mesoporous hybrid silica nanoparticles as carrier systems. *Nano Lett* **9**: 3308–3311.
28. Liong, M, Lu, J, Kovochich, M, Xia, T, Ruehm, SG, Nel, AE *et al.* (2008). Multifunctional inorganic nanoparticles for imaging, targeting, and drug delivery. *ACS Nano* **2**: 889–896.
29. Efferson, CL, Winkelmann, CT, Ware, C, Sullivan, T, Giampaoli, S, Tammam, J *et al.* (2010). Downregulation of Notch pathway by a gamma-secretase inhibitor attenuates AKT/mammalian target of rapamycin signaling and glucose uptake in an ERBB2 transgenic breast cancer model. *Cancer Res* **70**: 2476–2484.
30. Pece, S, Serresi, M, Santolini, E, Capra, M, Hulleman, E, Galimberti, V *et al.* (2004). Loss of negative regulation by Numb over Notch is relevant to human breast carcinogenesis. *J Cell Biol* **167**: 215–221.
31. Sahlgren, C, Gustafsson, MV, Jin, S, Poellinger, L and Lendahl, U (2008). Notch signaling mediates hypoxia-induced tumor cell migration and invasion. *Proc Natl Acad Sci USA* **105**: 6392–6397.
32. Lu, J, Liong, M, Li, Z, Zink, JI and Tamanoi, F (2010). Biocompatibility, biodistribution, and drug-delivery efficiency of mesoporous silica nanoparticles for cancer therapy in animals. *Small* **6**: 1794–1805.
33. Fre, S, Pallavi, SK, Huyghe, M, Laé, M, Janssen, KP, Robine, S *et al.* (2009). Notch and Wnt signals cooperatively control cell proliferation and tumorigenesis in the intestine. *Proc Natl Acad Sci USA* **106**: 6309–6314.
34. Fre, S, Huyghe, M, Mourikis, P, Robine, S, Louvard, D and Artavanis-Tsakonas, S (2005). Notch signals control the fate of immature progenitor cells in the intestine. *Nature* **435**: 964–968.
35. Dong, Y, Li, A, Wang, J, Weber, JD and Michel, LS (2010). Synthetic lethality through combined Notch-epidermal growth factor receptor pathway inhibition in basal-like breast cancer. *Cancer Res* **70**: 5465–5474.
36. Maeda, H (2010). Tumor-selective delivery of macromolecular drugs via the EPR effect: background and future prospects. *Bioconjug Chem* **21**: 797–802.
37. Tsai, C-P, Chen, C-Y, Hung, Y, Chang, F-H and Mou, C-Y (2009). Monoclonal antibody-functionalized mesoporous silica nanoparticles (MSN) for selective targeting breast cancer cells. *J Mater Chem* **19**: 5737–5743.
38. Zhu, C-L, Song, X-Y, Zhou, W-H, Yang, H-H, Wen, Y-H and Wang X-R (2009). An efficient cell-targeting and intracellular controlled-release drug delivery system based on MSN-PEM-aptamer conjugates. *J Mater Chem* **41**: 7765–7770.
39. Burns, AA, Vider, J, Ow, H, Herz, E, Penate-Medina, O, Baumgart, M *et al.* (2009). Fluorescent silica nanoparticles with efficient urinary excretion for nanomedicine. *Nano Lett* **9**: 442–448.
40. Souris, JS, Lee, CH, Cheng, SH, Chen, CT, Yang, CS, Ho, JA *et al.* (2010). Surface charge-mediated rapid hepatobiliary excretion of mesoporous silica nanoparticles. *Biomaterials* **31**: 5564–5574.
41. Nakamura, T, Yamada, Y and Yano, K (2007). Direct synthesis of monodispersed thiol-functionalized nanoporous silica spheres and their application to a colloidal crystal embedded with gold nanoparticles. *J Mater Chem* **17**: 3726–3732.